Fabrication of Dental Crown by Optical Coherence Tomography: A Pilot Study

SANGBONG LEE[1], KEUNBADA SON[2,3], JAEYUL LEE[1], MANSIK JEON[1], (Member, IEEE), KYU-BOK LEE[2,4], AND JEEHYUN KIM[1], (Member, IEEE)

[1]School of Electronics Engineering, College of IT Engineering, Kyungpook National University, Daegu 41566, South Korea
[2]Advanced Dental Device Development Institute, Kyungpook National University, Daegu 41940, South Korea
[3]Department of Dental Science, Graduate School, Kyungpook National University, Daegu 41940, South Korea
[4]Department of Prosthodontics, School of Dentistry, Kyungpook National University, Daegu 41940, South Korea

Corresponding authors: Mansik Jeon (msjeon@knu.ac.kr) and Kyu-Bok Lee (kblee@knu.ac.kr)

ABSTRACT Digital impressions have been studied for better gingival retraction in including the under subgingival finish line condition. Here, we employed swept-source optical coherence tomography (SS-OCT) of 1310 nm wavelength, which is capable of noninvasive, high-resolution, and high-speed, to discern the utilization-possibility for supporting the fabrication of the dental crown. A three-dimensional (3D) abutment was used at the 0.5 mm of the subgingival finish line below the level of the gingiva. The SS-OCT system scanned a field of view of 10 mm × 10 mm using the 3D working model by the depth-directional three focal points. The obtained 1500 images of OCT cross-sections, which are 1221 × 1220 pixels, were rendered to the 3D model for the effective design of a virtual crown. Then, the ceramic crown was fabricated through a milling machine with a computer-aided design and computer-aided manufacturing (CAD/CAM) software. The marginal fit of the crown was evaluated 219.1 ± 48.9 μm by a silicone replica technique. Although the marginal fit is not sufficient for the clinical allowable gap at one resin typodont, this study can be anticipated to encourage further researches for the enhanced fabrication of dental crown under subgingival finish line conditions.

INDEX TERMS Swept-source optical coherence tomography, virtual crown, subgingival scanning, two-dimensional image stack, three-dimensional modeling.

I. INTRODUCTION

Development of computer graphics has led to various applications of the computer-aided design and computer-aided manufacturing (CAD/CAM) system. In the field of dentistry, CAD/CAM is used for planning and manufacturing dental restorations [1]–[4]. The introduction of dental CAD/CAM has allowed accurate restoration with superior comfort and patient's preferences than the conventional method, and reduced probability of cross-infection [5]–[7]. Restorations using dental CAD/CAM have been accomplished with digital impressions. Digital impressions have been conducted

The associate editor coordinating the review of this manuscript and approving it for publication was Mohamad Forouzanfar.

by measuring the geometric shapes of the tooth in three dimensions using a dental scanner and converting the measurements into digital data [8]–[10]. Dental scanners have been used both as contact and noncontact types. Contact-type scanners are rarely used because of the slow scanning time and accuracy in the region of interest (ROI) where the sensor cannot contact based on the sensor of scanning the tooth surfaces. [11], [12]. In contrast, nowadays, noncontact-type scanners based on optical scanner are basically used in dentistry [13]–[15]. Complete workflows of fixed prosthesis with digital impressions are established using the intraoral scanner [16]–[18]. However, most commercial intraoral scanners allow scanning of only the tooth surface due to the optical scanner types. Gingival retraction is necessary to visualize the
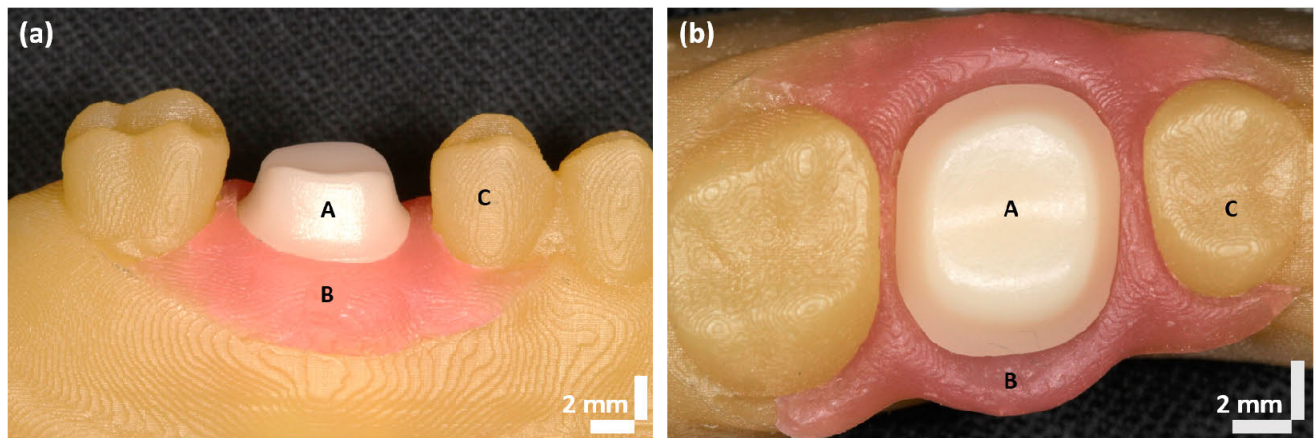
FIGURE 1. Photograph of a working model. (a) Buccal view, (b) Occlusal view. (A: Abutment fabricated with ceramic material, B: Artificial gingival with translucency, C: Adjacent teeth).

subgingival area with gingival displacement while intraoral scanners scan the abutment under the subgingival finish line condition [8], [19]. Scanning data can be sufficiently affected by several factors such as gingival sulcus bleeding, saliva, and periodontal condition of patients [10], [20]. Thus, scanning data are associated with problems such as reduced reliability and complexity of the scanning process caused due to the limitations of intraoral scanners [21].

Ultrasound has been proposed as an alternative to optical scanner because it can penetrate soft tissues without causing physical and biological damage. Therefore, it can scan the tooth under the subgingival finish line condition without gingival retraction [11], [22]. Digital impression using ultrasound is less affected by oral fluid and periodontal condition of patients [23], [24]. However, these methods have a major disadvantage, i.e., insufficient resolution and necessity of ultrasonic transmission media. Optical coherence tomography (OCT) has the capabilities of noncontact, noninvasive, nonionizing, and high-resolution scanning with various biomedical applications [25]–[28]. OCT has been well-utilized for various studies in dentistry such as for the detection of dental caries and gingival sulcus and the evaluation of dental abfraction and attrition [29]–[35]. In addition, quantitative assessment of dental treatments using OCT has been reported such as internal and marginal fitting of dental prosthesis and dental restoration [36]–[39].

Marginal and internal fit is the most important evaluation criteria for dental fixed prostheses [6], [36], [40]. With the recent advances in dental CAD/CAM systems, the marginal fit is a very low value within 100 μm, while most of the literature reports the clinically allowable marginal gap to be within a range of 100-120 μm [6], [36]. Since commercial intraoral scanners are difficult to scan the finish line is located under the gingiva [41], present study reported the possibility of prosthesis manufacturing after scanning with the OCT system. In this study, digital impression was accomplished using the swept-source OCT (SS-OCT) system to construct an accurate three-dimensional (3D) model. The CAD/CAM

software loaded the virtual crown after scanning the 3D working model of abutment using SS-OCT. Furthermore, the ceramic crown was fabricated by using a milling machine and the fit of the crown was evaluated by the silicone replica technique. The conceptual breakthrough of this study indicates high-resolution digital impression under the subgingival finish line condition.

II. MATERIALS AND METHODS
A. PREPARATION OF STUDY MODEL
A resin maxillary typodont (AG-3 ZPVK, Frasaco GmbH, Tettnang, Germany) was fabricated by 3D printing for fabricating the working model with an environment similar to that of actual teeth. And then the typodont was scanned by using the OCT system. The right first molar was prepared under the following conditions for the ceramic crown: subgingival position, depth of 1.2 mm in the chamfer form, and angle set at 6°. The prepared first molar was scanned by a laboratory scanner (E1, 3Sahpe, Copenhagen, Denmark). The scanning data of the abutment (prepared first molar) were transferred into the CAM software. Then, the abutment was fabricated with a ceramic material (IPS e.max CAD, Ivoclar Vivadent, Bendererstrasse, Liechtenstein) using a milling machine (Ezis HM, DDS, Seoul, South Korea). The ceramic material selected was lithium disilicate glass ceramic, considering transparency and color similar to those of actual teeth. Fig. 1 shows the photograph of the working model. The milled abutment was polished and crystallized. The resin typodont gingival around the abutment was removed. The removed resin typodont gingival was replaced by adding a little red color to the transparent polyvinylsiloxane impression material (ORTHO CLEAR, AMOC, Seoul, South Korea) for achieving color and translucency similar to actual gingival.

The abutment was fixed to the working model without movement so that the finish line could be placed at the subgingival finish line (0.5 mm below the level of the gingiva). The depth of the finish line was confirmed using a periodontal probe (CP 15 UNC, HU-Friedy, USA).
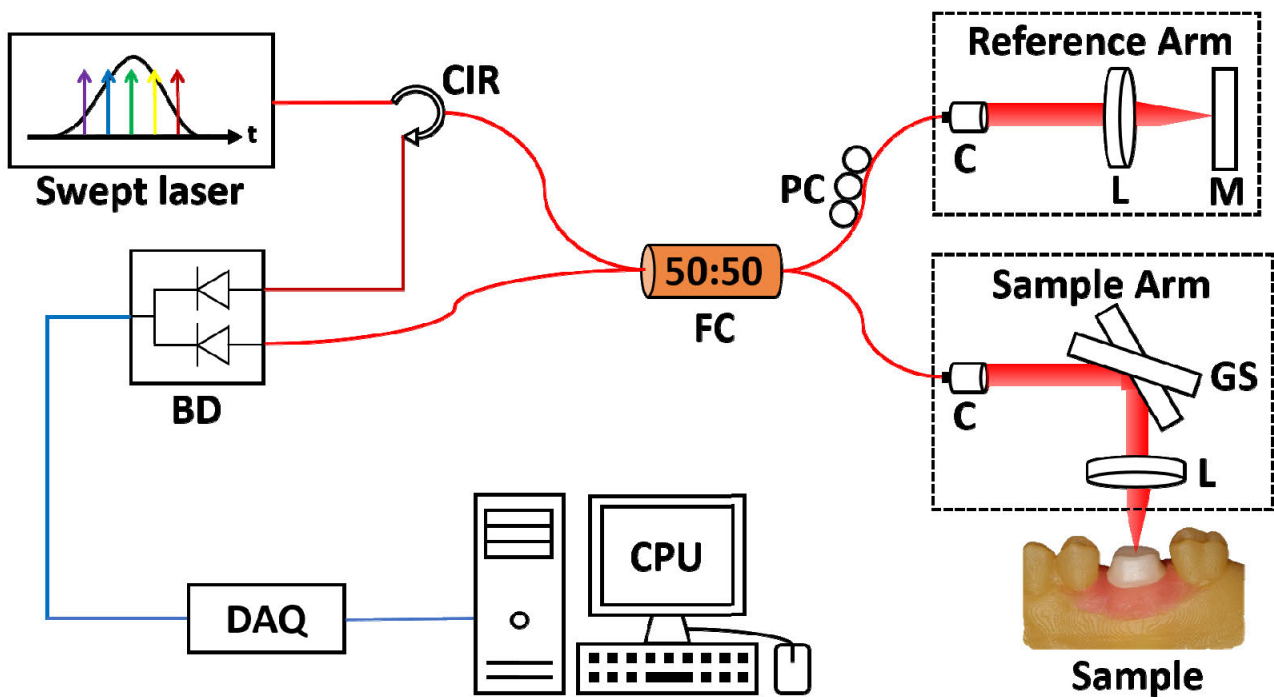
FIGURE 2. Schematic of the 1310-nm swept-source optical coherence tomography system. CIR: circulator; FC: fiber coupler; PC: polarization controller; C: collimator; L: lens; M: mirror; GS: galvanometer scanner; BD: balanced detector; DAQ: data acquisition card; CPU: central processing unit.

B. SS-OCT CONFIGURATION
The OCS1310V1 SS-OCT system (Thorlabs, Newton, USA) was used with a center wavelength of 1310 ± 15 nm, bandwidth of >97 nm, and average optical output power of 20 mW (Fig. 2). The OCT system has an axial scan line rate of 100 kHz and a sensitivity of 105 dB. In cross-sectional OCT image, it has an axial resolution of 16 μm and lateral resolution of 25 μm at the tissue level. The maximum dimensions of the OCT system are 10 mm × 10 mm × 12 mm. The OCT system scanned the working model located under the probe of the sample arm. The sample was moved using the plane two-axis linear stages. The light beam generated from the swept laser source was passed into a 50:50 fiber coupler. Then, the beam that passed into the fiber coupler was divided into two arms: reference and sample. The beam of the reference arm was reflected by a mirror, which entered the fiber coupler. Similarly, the beam of the sample arm was reflected by a sample, which entered the fiber coupler. The two reflected beams in the fiber coupler generated an interference signal. A balanced detector received the interference signal. The data acquisition card digitized the obtained signal. After these steps, the cross-sectional OCT image was acquired by reconstruction of the digitized signal [42], [43]. Further, OCT scanned the working model under a field of view of 10 mm × 10 mm. The obtained 2D OCT images were sized 1221 × 1220 pixels. The OCT system scanned the sample thrice by adjusting the focused position of the OCT image from top to bottom to implement a more accurate 3D model. A total of 1500 OCT 2D images was rendered from three-volume of each 500 2D stacks.
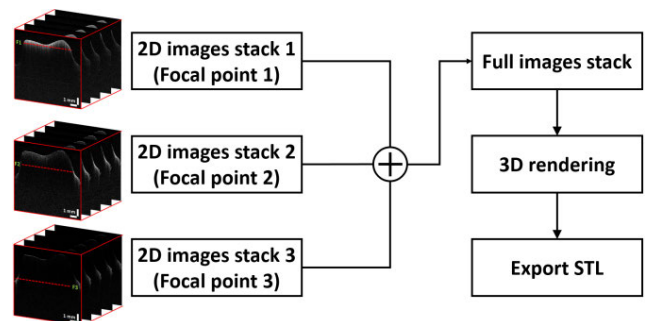

FIGURE 3. Algorithm of standard tessellation language exporting process from 2D image stacks.

C. 3D MODELING USING 2D IMAGE STACKS
Fig. 3 shows the STL exporting process from the 2D image stacks by the three different focal planes of axial directions. First, we obtained three image stacks by adjusting the focal length of the OCT system. The 2D image stacks acquired from three repetitions were combined to acquire full image stacks. The 2D images of the full image stacks were rearranged repeatedly in the following image order of focal points: 1, 2, and 3.

Regarding 3D rendering, we used the image processing software ImageJ (National Institutes of Health, Bethesda, MD, USA). The 2D images of the full image stacks were imported using ImageJ; then, 3D reconstruction was conducted using the 3D viewer from the Plugins menu of ImageJ. We set to export the STL format and reduced the noise in the 3D model by controlling the threshold of the software. The obtained 3D surface of the sample was exported in the STL format as the binary type.
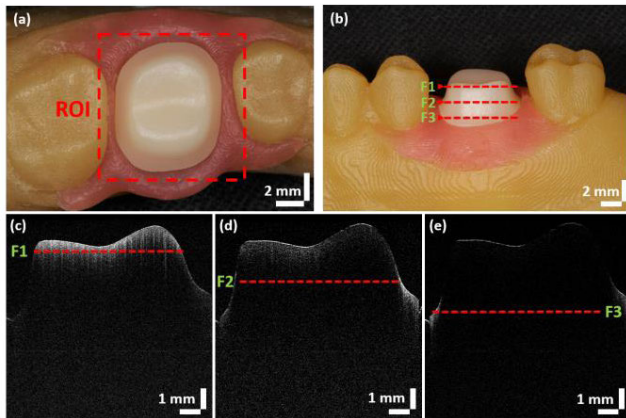
FIGURE 4. (a) Region of interest of sample in occlusal view (b) Focal points of abutment in buccal view (F1: Focal point 1, F2: Focal point 2, F3: Focal point 3), (c–e) Cross-sectional optical coherence tomography images of abutment using the three different focal points.

Finally, we smoothed and removed unnecessary sections of the STL file using several software such as Blender (Blender Foundation, Amsterdam, Netherlands) and Mesh-Lab (ICTI-CNR, Pisa, Italy). The STL file was loaded into the CAD software (Ezis VR, DDS, Seoul, South Korea), and the design of the virtual crown was modified using the CAD software. Next, the designed crown was loaded into the CAM software (Ezis VR, DDS) and fabricated by milling the ceramic block (Vita Suprinity, Vita Zahnfabrik, Bad Säckingen, Germany) using a milling machine (Ezis HM, DDS). For evaluating the accuracy of the 3D model obtained using OCT images, the fit of the crown was assessed by the silicone replica technique.

III. RESULTS

A. 2D IMAGE STACKS FOR 3D ABUTMENT MODEL

Sample photographs and 2D OCT images are presented in Fig. 4. The ROI of the working model is shown in Fig. 4(a). The three different focal points indicate the top, middle, and bottom points of the sample in Fig. 4(b). The top surface is more clearly scanned, but the bottom region is blurry at the focal point 1 of OCT, as shown in Fig. 4(c). The cross-sectional OCT images of the middle and bottom focal points, i.e., focal points 2 and 3, enhance the adjacent surface of the pillar and gingival boundary. The abutment OCT images of the three focal points improved the validity of surface performance, as shown in Fig. 4(c–e). Next, the obtained three 2D image stacks were combined and rearranged to acquire full image stacks. The full image stacks were imported and reconstructed to the 3D model.

B. DENTAL CAD/CAM PROCESS FOR THE CROWN

Fig. 5 shows the dental CAD process using 3D OCT data. The 3D abutment is illustrated with an STL file of OCT scanned using the CAD software, as shown in Fig. 5(a). The adjacent tooth was scanned using an intraoral scanner (i500, Medit, Seoul, South Korea). The abutment and adjacent tooth scanned data were merged using a 3D inspection software (Geomagic Control X; 3DSystems, Rock Hill,
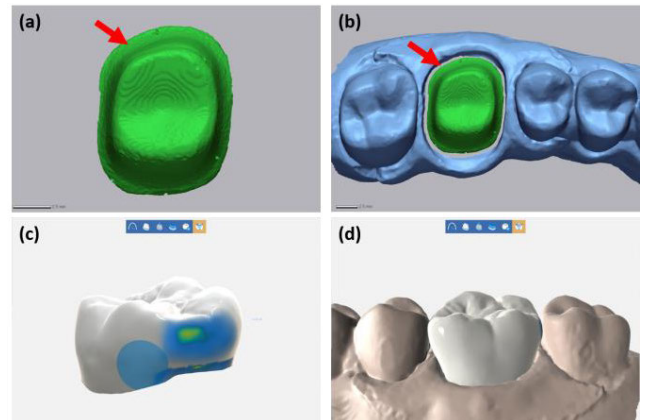

FIGURE 5. Dental computer-aided design process. (a) Acquisition of abutment optical coherence tomography (OCT) data, (b) merging with OCT data of abutment and adjacent teeth, (c) modification of prosthesis size and position, and (d) virtual crown.
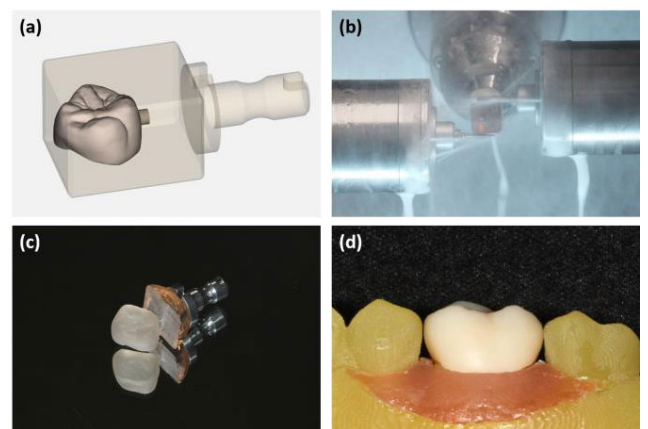

FIGURE 6. Dental computer-aided manufacturing process. (a) Crown position adjustment with ceramic block, (b) milling, (c) milled crown before crystallization, and (d) seated crown on working model.

SC, USA), as shown in Fig. 5(b). The red arrows in Fig. 5(a, b) indicate the sufficiently scanned subgingival finish line in OCT for stably maintaining the subgingival finish line condition at 0.5 mm below the level of the working model gingiva. The 3D abutment was accurately employed in line with the adjacent teeth on the CAD software. The CAD software was used to modify the prosthesis design to complete the crown. The modification of prosthesis size and position is visualized in Fig. 5(c). The virtual crown is positioned as shown in Fig. 5(d). The CAM process of virtual crown with the working model is illustrated in Fig. 6. The virtual crown, which is obtained by the CAD software, was loaded into the CAM software. The position of the virtual crown was corrected, and a connection was added on the ceramic block. The adjusted crown position is displayed on the ceramic block, as shown in Fig. 6(a). The ceramic block was milled through the milling machine. Milling and the milled crown before crystallization are shown in Fig. 6(b, c). The milled ceramic crown was removed and crystallized according to the recommendation of the manufacturer in a ceramic furnace (Programat EP 5000, IVoclar Vivadent). After polishing, the
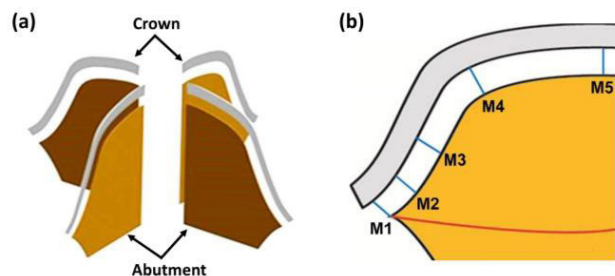
FIGURE 7. (a) Divided surface and (b) measurement point of the silicone replica (M1: marginal gap, M2: chamfer gap, M3: axial gap, M4: angle gap, M5: occlusal gap).

crown was applied on the working model. The seated crown on the working model was considered sufficient for practical application, as shown in Fig. 6(d).

C. SILICONE REPLICA TECHNIQUE FOR EVALUATION OF THE CROWN FITNESS

Most literature reports the clinically allowable marginal gap to be within 120 μm [6], [37]. The fit of the crown was evaluated by the silicone replica technique as a non-destructive method [6], [37]. Its inner surface was filled with light body impression materials (Aquasil Ultra Monophase, Dentsply Sirona, Konstanz, Germany) and carefully seated on the abutment of the working model. It was then confirmed that the crown was positioned correctly and loaded with finger pressure. Moreover, for stable cutting, the light body silicone was covered with medium body silicone (Aquasil Ultra Monophase, Dentsply Sirona). After polymerization of the medium body silicone, the silicone was cut using a razor blade (Personna, American Safety Razor, Staunton, Virginia, USA) in the mesiodistal and buccolingual directions. The images were captured at 160× magnification using an industrial video microscope system (IMS 1080P, SOMETECH, Seoul, South Korea). The captured images were loaded into ITPlus 5.0 (SOMETECH, Seoul, South Korea) that could measure the gap. Using the tools provided in the software, the position at which gap measurements would be desired was selected for crown and abutment, and marginal and internal gaps were measured as shown in Fig. 7.

The representative images show the gaps and measurement points in Fig. 7. The points of M1, M2, M3, M4, and M5 indicate the marginal gap, chamfer gap, axial gap, angle gap, and occlusal gap, respectively. Internal gaps were measured in the axial, angle, and occlusal areas. The discrepancy in marginal gaps was 219.1 ± 48.9 μm and that in internal gaps was 58.2 ± 30.4, 161.1 ± 52.2, and 463.7 ± 16.2 μm for the angle, axial, and occlusal areas.

IV. DISCUSSION

Commercially available intraoral scanners are limited to the surface imaging for the scanning of the abutment and periodontal area [44]. The oral-scanning image can offer topographic information but it has a low precision with low resolutions by the different scanning directions [45]. However, the OCT technique, which is capable of providing a noninvasive cross-sectional image with tomographic information, has a more high-resolution of several micro-scales compared to the intraoral scanners [39]. Moreover, OCT has a high precision that presents almost the consistent performance even by the different multiple users. Although OCT techniques have not been developed to rapidly scan the whole teeth compared with commercial oral-scanner, the technique will be considered as the supporting technique of oral scanning for high-accuracy 3D modeling [46], [47]. The depth-of-focus (DOF) of the OCT system has been difficult in covering the whole region of depth-directional scanning at one time. The 3D scanning of one focal point was difficult to acquire sufficient data for accurate 3D modeling due to the fixed DOF of the OCT system. Thus, the SS-OCT system scanned the sample by three focused positions with different focal points of top, middle, and bottom, to implement more accurate 3D modeling of the abutment. Especially, the accuracy of 3D modeling can be improved with more multiple focused scanning. The design of the OCT system can be modified for enhancement of possibility as an intraoral scanner in future works.

The 3D model of the depth of 0.5 mm below the level of the gingival was used for the scanning of dental abutment at the subgingival finish line, the OCT technique can sufficiently visualize the working model of the depth of more than 1.5 mm. The clinical significance of this study indicates the evaluation efficiency of the subgingival margin of the dental crown with keeping the biologic width and attractiveness of teeth through the restoration. This research indicates the results without consideration of gingival biotypes as a preliminary study. The variability of gingival biotypes will be divided into thick biotype or thin biotype. The OCT technique also is needed to be specifically developed by the respective biotypes with the enhancement of penetration depth or resolutions for the precisely designed experiment. The aim of this study is to show the utilization possibility of the SS-OCT system to scan the 3D model of abutment for the fabrication of dental crown under the subgingival finish line condition. Although, the one sample of resin typodont was used without controls, the experiment sufficiently carried out the process of dental fabrication with the OCT technique and CAD/CAM software. The discrepancy of marginal gaps and occlusal internal gaps was so high for biological tissues, which was 219.1 ± 48.9 μm and 463.7 ± 16.2 μm, respectively. The values of one sample couldn't represent the clinical reality. The marginal and internal fit of the crown produced through the scanning method presented showed inaccuracy. This inaccuracy is related to the quality of 3D modeling acquired through scanning [6], [39]. The SS-OCT system was utilized to accomplish the scanning of the marginal region under the gingiva, which was different from the purpose of scanning precision on the tooth surface with a conventional intraoral scanner. Ultimately, it is necessary to optimize the method of processing the image to enhance the quality including the precise scanning of tooth surface that can be compared to conventional intraoral scanners.

V. CONCLUSION

The SS-OCT system with a 1310-nm wavelength was used to visualize the abutment of a working model, which had a sulcus length of 0.5 mm. The 3D modeling of OCT images was enhanced by three focal point scanning in the axial direction for better accuracy using the customized rendering algorithm. Dental crown was fabricated using the CAD/CAM system and milled for application in the working model. Based on one sample, the measured discrepancy of marginal gaps and internal gaps was difficult to reach a clinical reality for potential dental scan. Although the marginal and internal fits were not sufficient for use in clinical application, the SS-OCT system represents the novel evaluation under the subgingival finish line condition with properties of noninvasiveness, high-resolution, and high-speed. Therefore, the proposed method can be variously utilized to support the further researches including the consideration of biotypes for clinical employment.

REFERENCES

[1] T. F. Alghazzawi, "Advancements in CAD/CAM technology: Options for practical implementation," *J. Prosthodontic Res.*, vol. 60, no. 2, pp. 72–84, Apr. 2016.

[2] J. Abduo, K. Lyons, and M. Bennamoun, "Trends in computer-aided manufacturing in prosthodontics: A review of the available streams," *Int. J. Dentistry*, vol. 2014, pp. 1–15, Jan. 2014.

[3] R. van Noort, "The future of dental devices is digital," *Dental Mater.*, vol. 28, no. 1, pp. 3–12, Jan. 2012.

[4] T. Miyazaki and Y. Hotta, "CAD/CAM systems available for the fabrication of crown and bridge restorations," *Austral. Dental J.*, vol. 56, pp. 97–106, Jun. 2011.

[5] B. C. Spies, S. Witkowski, K. Vach, and R.-J. Kohal, "Clinical and patient-reported outcomes of zirconia-based implant fixed dental prostheses: Results of a prospective case series 5 years after implant placement," *Clin. Oral Implants Res.*, vol. 29, no. 1, pp. 91–99, Jan. 2018.

[6] M. Vojdani, K. Torabi, E. Farjood, and A. A. R. Khaledi, "Comparison the marginal and internal fit of metal copings cast from wax patterns fabricated by CAD/CAM and conventional wax up techniques," *J. Dentistry*, vol. 14, p. 118, Sep. 2013.

[7] F. Nejatidanesh, H. Moradpoor, and O. Savabi, "Clinical outcomes of zirconia-based implant- and tooth-supported single crowns," *Clin. Oral Investigations*, vol. 20, no. 1, pp. 169–178, Jan. 2016.

[8] S. Ting-shu and S. Jian, "Intraoral digital impression technique: A review," *J. Prosthodontics*, vol. 24, no. 4, pp. 313–321, Jun. 2015.

[9] P. Seelbach, C. Brueckel, and B. Wöstmann, "Accuracy of digital and conventional impression techniques and workflow," *Clin. Oral Investigations*, vol. 17, no. 7, pp. 1759–1764, Sep. 2013.

[10] A. Syrek, G. Reich, D. Ranftl, C. Klein, B. Cerny, and J. Brodesser, "Clinical evaluation of all-ceramic crowns fabricated from intraoral digital impressions based on the principle of active wavefront sampling," *J. Dentistry*, vol. 38, no. 7, pp. 553–559, Jul. 2010.

[11] L. Praça, F. C. Pekam, R. O. Rego, K. Radermacher, S. Wolfart, and J. Marotti, "Accuracy of single crowns fabricated from ultrasound digital impressions," *Dental Mater.*, vol. 34, no. 11, pp. e280–e288, Nov. 2018.

[12] S. Fukazawa, C. Odaira, and H. Kondo, "Investigation of accuracy and reproducibility of abutment position by intraoral scanners," *J. Prosthodontic Res.*, vol. 61, no. 4, pp. 450–459, Oct. 2017.

[13] W.-S. Lee, J.-K. Park, J.-H. Kim, H.-Y. Kim, W.-C. Kim, and C.-H. Yu, "New approach to accuracy verification of 3D surface models: An analysis of point cloud coordinates," *J. Prosthodontic Res.*, vol. 60, no. 2, pp. 98–105, Apr. 2016.

[14] R. Richert, A. Goujat, L. Venet, G. Viguie, S. Viennot, P. Robinson, J.-C. Farges, M. Fages, and M. Ducret, "Intraoral scanner technologies: A review to make a successful impression," *J. Healthcare Eng.*, vol. 2017, pp. 1–9, Jan. 2017.

[15] C. Goracci, L. Franchi, A. Vichi, and M. Ferrari, "Accuracy, reliability, and efficiency of intraoral scanners for full-arch impressions: A systematic review of the clinical evidence," *Eur. J. Orthodontics*, vol. 38, no. 4, pp. 422–428, Aug. 2016.

[16] T. Joda, F. Zarone, and M. Ferrari, "The complete digital workflow in fixed prosthodontics: A systematic review," *BMC Oral Health*, vol. 17, no. 1, p. 124, Dec. 2017.

[17] J.-Y. Sim, Y. Jang, W.-C. Kim, H.-Y. Kim, D.-H. Lee, and J.-H. Kim, "Comparing the accuracy (trueness and precision) of models of fixed dental prostheses fabricated by digital and conventional workflows," *J. Prosthodontic Res.*, vol. 63, no. 1, pp. 25–30, Jan. 2019.

[18] Y. Takeuchi, H. Koizumi, M. Furuchi, Y. Sato, C. Ohkubo, and H. Matsumura, "Use of digital impression systems with intraoral scanners for fabricating restorations and fixed dental prostheses," *J. Oral Sci.*, vol. 60, no. 1, pp. 1–7, 2018.

[19] M. Boeddinghaus, E. S. Breloer, P. Rehmann, and B. Wöstmann, "Accuracy of single-tooth restorations based on intraoral digital and conventional impressions in patients," *Clin. Oral Investigations*, vol. 19, no. 8, pp. 2027–2034, Nov. 2015.

[20] T. V. Flügge, S. Schlager, K. Nelson, S. Nahles, and M. C. Metzger, "Precision of intraoral digital dental impressions with iTero and extraoral digitization with the iTero and a model scanner," *Amer. J. Orthodontics Dentofacial Orthopedics*, vol. 144, no. 3, pp. 471–478, Sep. 2013.

[21] R. G. Nedelcu and A. S. K. Persson, "Scanning accuracy and precision in 4 intraoral scanners: An in vitro comparison based on 3-dimensional analysis," *J. Prosthetic Dentistry*, vol. 112, no. 6, pp. 1461–1471, Dec. 2014.

[22] J. Marotti, S. Heger, J. Tinschert, P. Tortamano, F. Chuembou, K. Radermacher, and S. Wolfart, "Recent advances of ultrasound imaging in dentistry—A review of the literature," *Oral Surgery, Oral Med., Oral Pathol. Oral Radiol.*, vol. 115, no. 6, pp. 819–832, Jun. 2013.

[23] F. Chuembou Pekam, J. Marotti, S. Wolfart, J. Tinschert, K. Radermacher, and S. Heger, "High-frequency ultrasound as an option for scanning of prepared teeth: An *in vitro* study," *Ultrasound Med. Biol.*, vol. 41, no. 1, pp. 309–316, Jan. 2015.

[24] K. Degen, D. Habor, K. Radermacher, S. Heger, J.-S. Kern, S. Wolfart, and J. Marotti, "Assessment of cortical bone thickness using ultrasound," *Clin. Oral Implants Res.*, vol. 28, no. 5, pp. 520–528, May 2017.

[25] J. Lee, R. E. Wijesinghe, D. Jeon, P. Kim, Y.-H. Choung, J. H. Jang, M. Jeon, and J. Kim, "Clinical utility of intraoperative tympanomastoidectomy assessment using a surgical microscope integrated with an optical coherence tomography," *Sci. Rep.*, vol. 8, no. 1, pp. 1–8, Dec. 2018.

[26] W. Drexler, M. Liu, A. Kumar, T. Kamali, A. Unterhuber, and R. A. Leitgeb, "Optical coherence tomography today: Speed, contrast, and multimodality," *J. Biomed. Opt.*, vol. 19, no. 7, Jul. 2014, Art. no. 071412.

[27] J. Lee, K. Kim, R. E. Wijesinghe, D. Jeon, S. H. Lee, M. Jeon, and J. H. Jang, "Decalcification using ethylenediaminetetraacetic acid for clear microstructure imaging of cochlea through optical coherence tomography," *J. Biomed. Opt.*, vol. 21, no. 8, Mar. 2016, Art. no. 081204.

[28] B. Jeon, J. Lee, D. Jeon, P. Kim, J. H. Jang, R. E. Wijesinghe, M. Jeon, and J. Kim, "Functional assessment of moisture influenced cadaveric tympanic membrane using phase shift-resolved optical Doppler vibrography," *J. Biophotonics*, vol. 13, no. 2, Feb. 2020, Art. no. e201900202.

[29] Y. Shimada, A. Sadr, Y. Sumi, and J. Tagami, "Application of optical coherence tomography (OCT) for diagnosis of caries, cracks, and defects of restorations," *Current Oral Health Rep.*, vol. 2, no. 2, pp. 73–80, Jun. 2015.

[30] H. T. Lakshmikantha, N. K. Ravichandran, M. Jeon, J. Kim, and H.-S. Park, "3-dimensional characterization of cortical bone microdamage following placement of orthodontic microimplants using optical coherence tomography," *Sci. Rep.*, vol. 9, no. 1, pp. 1–13, Dec. 2019.

[31] J. Lee, J. Park, M. Faizan Shirazi, H. Jo, P. Kim, R. E. Wijesinghe, M. Jeon, and J. Kim, "Classification of human gingival sulcus using swept-source optical coherence tomography: *in vivo* imaging," *Infr. Phys. Technol.*, vol. 98, pp. 155–160, May 2019.

[32] L. O. Fernandes, C. C. B. O. Mota, L. S. A. de Melo, M. U. S. da Costa Soares, D. da Silva Feitosa, and A. S. L. Gomes, "*In vivo* assessment of periodontal structures and measurement of gingival sulcus with optical coherence tomography: A pilot study," *J. Biophotonics*, vol. 10, pp. 862–869, Jun. 2017.

[33] N. K. Ravichandran, H. Cho, J. Lee, S. Han, R. E. Wijesinghe, P. Kim, J.-W. Song, M. Jeon, and J. Kim, "An averaged intensity difference detection algorithm for identification of human gingival sulcus in optical coherence tomography images," *IEEE Access*, vol. 7, pp. 73076–73084, 2019.

[34] C. Marcauteanu, A. Bradu, C. Sinescu, F. I. Topala, M. L. Negrutiu, and A. G. Podoleanu, "Quantitative evaluation of dental abfraction and attrition using a swept-source optical coherence tomography system," *J. Biomed. Opt.*, vol. 19, no. 2, Sep. 2013, Art. no. 021108.

[35] J. Lee, S. Han, J. Hwang, S. Park, D. Jeon, K. Kim, R. E. Wijesinghe, K.-B. Lee, M. Jeon, and J. Kim, "Identification of multi-dimensional thread geometry using depth-resolved swept-source optical coherence tomography for assessment of dental implant fabrication," *Opt. Lasers Eng.*, vol. 127, Apr. 2020, Art. no. 105951.

[36] J. T. Colpani, M. Borba, and Á. Della Bona, "Evaluation of marginal and internal fit of ceramic crown copings," *Dental Mater.*, vol. 29, no. 2, pp. 174–180, Feb. 2013.

[37] S.-H. Han, A. Sadr, J. Tagami, and S.-H. Park, "Non-destructive evaluation of an internal adaptation of resin composite restoration with swept-source optical coherence tomography and micro-CT," *Dental Mater.*, vol. 32, no. 1, pp. e1–e7, Jan. 2016.

[38] K. Kikuchi, N. Akiba, A. Sadr, Y. Sumi, J. Tagami, and S. Minakuchi, "Evaluation of the marginal fit at implant–abutment interface by optical coherence tomography," *J. Biomed. Opt.*, vol. 19, no. 5, May 2014, Art. no. 055002.

[39] S. Lee, K. Son, J. Park, J. Lee, S. H. Kang, R. E. Wijesinghe, P. Kim, J. H. Hwang, S. Park, B.-J. Yun, M. Jeon, K.-B. Lee, and J. Kim, "Nonionized, high-resolution measurement of internal and marginal discrepancies of dental prosthesis using optical coherence tomography," *IEEE Access*, vol. 7, pp. 6209–6218, 2019.

[40] K.-B. Kim, W.-C. Kim, H.-Y. Kim, and J.-H. Kim, "An evaluation of marginal fit of three-unit fixed dental prostheses fabricated by direct metal laser sintering system," *Dental Mater.*, vol. 29, no. 7, pp. e91–e96, Jul. 2013.

[41] R. Nedelcu, P. Olsson, I. Nyström, and A. Thor, "Finish line distinctness and accuracy in 7 intraoral scanners versus conventional impression: An *in vitro* descriptive comparison," *BMC Oral Health*, vol. 18, no. 1, p. 27, Dec. 2018.

[42] S. Aumann, S. Donner, J. Fischer, and F. Müller, "Optical coherence tomography (OCT): Principle and technical realization," in *High Resolution Imaging in Microscopy and Ophthalmology*. Cham, Switzerland: Springer, 2019, pp. 59–85.

[43] D. P. Popescu, C. Flueraru, Y. Mao, S. Chang, J. Disano, S. Sherif, and M. G. Sowa, "Optical coherence tomography: Fundamental principles, instrumental designs and biomedical applications," *Biophys. Rev.*, vol. 3, p. 155, Sep. 2011.

[44] S. B. M. Patzelt, A. Emmanouilidi, S. Stampf, J. R. Strub, and W. Att, "Accuracy of full-arch scans using intraoral scanners," *Clin. Oral Investigations*, vol. 18, no. 6, pp. 1687–1694, Jul. 2014.

[45] P. Medina-Sotomayor, M. A. Pascual, and A. I. Camps, "Accuracy of four digital scanners according to scanning strategy in complete-arch impressions," *PLoS ONE*, vol. 13, no. 9, Sep. 2018, Art. no. e0202916.

[46] N. K. Ravichandran, R. E. Wijesinghe, M. F. Shirazi, K. Park, M. Jeon, W. Jung, and J. Kim, "Depth enhancement in spectral domain optical coherence tomography using bidirectional imaging modality with a single spectrometer," *J. Biomed. Opt.*, vol. 21, no. 7, Jul. 2016, Art. no. 076005.

[47] Y. S. Hsieh, Y. C. Ho, S. Y. Lee, C. C. Chuang, J. C. Tsai, K. F. Lin, and C. W. Sun, "Dental optical coherence tomography," *Sensors*, vol. 13, no. 7, pp. 8928–8949, Jul. 2013.

KEUNBADA SON received the M.S. degree in dental science from Kyungpook National University, Daegu, South Korea, in 2019, where he is currently pursuing the Ph.D. degree with the School of Dentistry. He is also a Senior Researcher with the Advanced Dental Device Development Institute, Kyungpook National University. His research interests include dental science, digital dentistry, development of dental device, prosthodontics, and dental computer-aided design/computer-aided manufacturing systems.

JAEYUL LEE is currently pursuing the Ph.D. degree with the School of Electronics Engineering, Kyungpook National University, Daegu, South Korea. His research interests include development of high-resolution novel imaging techniques and optical imaging techniques, including photoacoustic microscopy, optical coherence tomography, optical coherence angiography, and handheld instruments and their biomedical applications.

MANSIK JEON (Member, IEEE) received the Ph.D. degree in electronics engineering from Kyungpook National University, Daegu, South Korea, in 2011. He is currently an Associate Professor with the School of Electronics Engineering, Kyungpook National University. His research interests include development of nonionizing and noninvasive novel biomedical imaging techniques, including photoacoustic tomography, photoacoustic microscopy, optical coherence tomography, ultrasonic imaging, and handheld scanner and their clinical applications.

KYU-BOK LEE received the Ph.D. degree in dentistry from Chonbuk National University, Jeonju, South Korea, in 2007. He is currently a Professor with the School of Dentistry, Kyungpook National University. His research interests include development of dental devices and materials, including 3D scanner, CAD/CAM, 3D print, implant, and ceramic and their clinical applications.

SANGBONG LEE received the B.E. degree in electronics engineering from Kyungpook National University, Daegu, South Korea, in 2018. He is currently a M.S. Researcher with the Electronics Engineering Department, Kyungpook National University. His research interests include development of optical system for biomedical application and biomedical imaging, including optical coherence tomography and photoacoustic microscopy.

JEEHYUN KIM (Member, IEEE) received the Ph.D. degree in biomedical engineering from The University of Texas at Austin, USA, in 2004. He was a Postdoctoral Researcher with the Beckman Laser institute, University of California, Irvine. He is currently a Professor with Kyungpook National University, Daegu, South Korea. His research interests include biomedical imaging and sensing, neuroscience studies using multiphoton microscopy, photo-acoustic imaging, and other novel applications of sensors.

• • •